

Mid-infrared Continuous-wave Optical Parametric Oscillator with a Fan-out Grating MgO:PPLN Operating Up to 5.3 μm

In-Ho Bae^{1,2}, Jae-Keun Yoo¹, Sun Do Lim¹, Seung Kwan Kim², and Dong-Hoon Lee^{1,2*}

¹Division of Physical Metrology, Korea Research Institute of Standards and Science, Daejeon 34113, Korea

²Quantum Technology Institute, Korea Research Institute of Standards and Science, Daejeon 34113, Korea

(Received August 26, 2019 : revised October 16, 2019 : accepted October 18, 2019)

We report on a continuous-wave (cw) optical parametric oscillator (OPO) optimized for mid-infrared emission above 5.0 μm . The OPO is based on a magnesium-oxide-doped periodically poled LiNbO₃ (MgO:PPLN) crystal with a fan-out grating design. A linear two-mirror cavity resonating both at the pump and signal wavelengths is stabilized to the pump laser by using the modified Pound-Drever-Hall (PDH) method. The idler wavelength is continuously tunable from 4.7 μm up to 5.3 μm by varying the poling period of the fan-out grating crystal. Pumped by a diode-pumped solid state (DPSS) laser with a power of 1.1 W at 1064 nm, the maximum idler output power is measured to be 5.3 mW at 4.8 μm . The output power above 5.0 μm is reduced to the hundreds of μW level due to increased absorption in the crystal, but is stable and strong enough to be measured with a conventional detector.

Keywords : Optical parametric oscillator, Mid-infrared laser, PPLN crystals

OCIS codes : (190.4410) Nonlinear optics, parametric processes; (190.4970) Parametric oscillators and amplifiers; (140.3070) Infrared and far-infrared lasers

I. INTRODUCTION

Since the first demonstration of the optical parametric oscillator (OPO) in 1965 [1], a variety of OPOs have been developed as a promising wavelength-tunable coherent light source covering a wide range from ultraviolet (UV) [2] to far-infrared [3]. In particular, the introduction of a quasi-phase matching (QPM) technique based on periodically poled nonlinear crystals [4] has accelerated the development in the past two decades. Among others, the periodically poled LiNbO₃ (PPLN) is established as the most efficient crystal for OPOs in many aspects: high nonlinearity in the preferred poling direction [5], easy and reliable fabrication of poling by using high voltage pulse [4], easy engineering of period pattern based on spatial masking [6], and availability of high-quality crystals for various applications [7-9].

PPLN crystals are, in particular, well suited for the continuous-wave (cw) OPOs, as the phase-matching can be realized along a long crystal to reduce the oscillation

threshold [10]. Moreover, PPLN provides a promising strategy for motor-controlled wide wavelength-tuning through engineering of poling patterns such as a fan-out grating design [11]. We are particularly interested in a cw OPO tunable in a wide wavelength range in the mid-infrared, where the molecular fingerprint of atoms and molecules can be detected by high-resolution laser spectroscopy [12]. Recent mid-infrared studies have led to the urgent need for the development of broadly tunable, narrow linewidth light sources as the demand in remote sensing applications such as defense science, biomedical spectroscopy, and gas sensing increases rapidly [13-16]. For example, gas sensing systems contain various absorption lines with a variety of molecules, such as methane (CH₄), carbon monoxide (CO), trioxxygen (O₃), nitrogen dioxide (NO₂), sulfur dioxide (SO₂) and formaldehyde (CH₂O). In order to cover the fundamental vibrational mode of these atmospheric constituents, a wide wavelength tuning of a mid-IR light source must be guaranteed [13, 14]. In the biomedical science, a molecular

*Corresponding author: dh.lee@kriss.re.kr, ORCID 0000-0003-3317-1415

Color versions of one or more of the figures in this paper are available online.



This is an Open Access article distributed under the terms of the Creative Commons Attribution Non-Commercial License (<http://creativecommons.org/licenses/by-nc/4.0/>) which permits unrestricted non-commercial use, distribution, and reproduction in any medium, provided the original work is properly cited.

spectroscopy using tunable mid-infrared light sources can be used for surgical and non-surgical operation [15]. In addition to the atomic and molecular spectroscopic applications mentioned above, high transmittance bands of the atmospheric gases also have prominent results in defense science and earth observation [16]. In particular, since the wavelength of the light emitted from the earth's surface or the missile contains the strong mid-infrared region, mid-IR applications are very useful for monitoring distant objects or features at night. In order to successfully perform gas sensing and defense science, which are important applications in the mid-infrared region, it is very important to develop a multi-purpose light source that can adjust not only a high absorption band but also a high transmission band. Therefore, cw OPO can be a good solution to the demand for mid-infrared light sources. However, obtaining a wavelength longer than $4.0\ \mu\text{m}$ from the cw OPO has been limited due to the increasing absorption of PPLN above $4.0\ \mu\text{m}$, which results in the increased oscillation threshold [17]. In addition, the stronger thermal effect of the PPLN crystal in association with the stronger absorption can prevent a cw OPO from stable operation at higher pump power [18]. Despite such difficulties, cw singly resonant OPOs (SROs) with ring cavity design have been reported on the long wavelengths more than $5.0\ \mu\text{m}$. Those results were achievable with multi-grating PPLN and high power lasers of several watts [19, 20]. On the other hand, pump resonant cavity design, so called pump-enhanced cavity, has a benefit for achieving lower oscillation threshold with excellent frequency tuning [21]. Based on a pump resonant cavity scheme, tunable operation from $4.0\ \mu\text{m}$ to $5.26\ \mu\text{m}$ of cw OPO was confirmed with multi-grating PPLN pumped by hundreds of mW [22]. For a pulsed OPO, for comparison, operation with a PPLN crystal is reported at a wavelength as long as $7.3\ \mu\text{m}$ [23].

In this work, we report on the direct measurement of the idler wavelength above $5.0\ \mu\text{m}$ by using a Fourier-transform infrared (FTIR) spectrometer and the output power in step of pump power with a calibrated HgCdTe detector. By using a 5 mol% magnesium-oxide-doped PPLN (MgO:PPLN) crystal (HC photonics) with a fan-out poling period from $24\ \mu\text{m}$ to $28\ \mu\text{m}$, the idler wavelength of the cw OPO is continuously tuned from $4.7\ \mu\text{m}$ to $5.3\ \mu\text{m}$. This scheme has the advantage that the wavelength tuning can be performed faster than those of OPOs with multi-grating PPLN, which causes wavelength tuning through temperature control. Our strategy for extending the wavelength range was to optimize the design of the OPO cavity for the stable operation. We used a two-mirror linear cavity that is resonant both for the pump and signal waves. Such a pump-enhanced design is effective to achieve the low oscillation threshold so that a pump laser with only moderate pump power can be used [24, 25]. In this experiment, the operating thresholds for producing long wavelengths more than $5.0\ \mu\text{m}$ were hundreds of mW. The moderate pump power is advantageous to reduce the thermal effect by

absorption of the pump power in the crystal. After the OPO oscillation, imperfect clampings of the intracavity pump power result from the thermal effect [26, 27]. In addition, the cavity stabilization is optimized for controlling the instability induced by absorption of the long-wavelength idler power. We applied the modified Pound-Drever-Hall (PDH) scheme for cavity stabilization, which is modified to directly modulate the pump laser frequency [28].

II. EXPERIMENTAL SETUP

The experimental schematics of the cw OPO oscillating above $5.0\ \mu\text{m}$ is shown in Fig. 1. We used a cw diode pumped solid state (DPSS) Nd:YAG laser (Mephisto, Coherent) at $1064\ \text{nm}$ as a pump source, with a linewidth of $1\ \text{kHz}$ and a maximum power of up to $1.1\ \text{W}$. The unwanted optical feedback into the pump laser is blocked by an optical isolator (ISO) placed in front of the laser. The beam of the pump laser aligned by two high reflectivity (HR) mirrors is incident into the OPO cavity after passing through the half-wave plate (HWP). In order to match the mode of the incident pump laser to the resonant cavity mode, a lens L1 with focal length of $120\ \text{mm}$ is used. Another lens L2 with focal length of $100\ \text{mm}$ collimates the emitted light from the cavity. Cavity mirrors M1 and M2 made on zinc selenide (ZnSe) substrates have the plano-concave shape with a radius of curvature of $-50\ \text{mm}$ and the high transmission at the idler wavelength ($T > 85\%$). The concave side of input mirror M1 is coated for high reflectivity ($R > 99\%$) for the signal wave and 5% transmission for the pump wave. The output mirror M2 has 2% transmission for the signal wave and high reflectivity ($R > 99\%$) for the pump wave. The backsides of the mirrors have a wedged cut to avoid additional resonance induced from the surface reflection of the pump and signal waves.

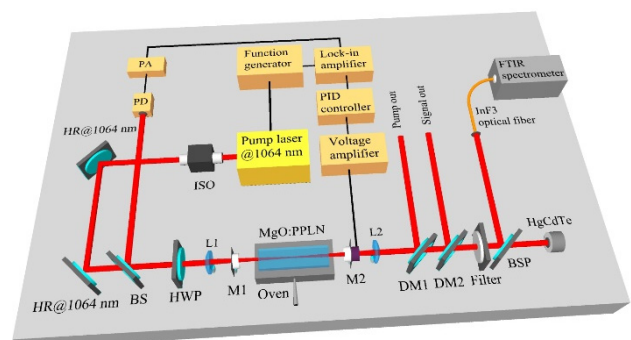


FIG. 1. The experimental schematics of MgO:PPLN-based mid-infrared continuous-wave OPO oscillating above $5.0\ \mu\text{m}$: ISO, isolator; HR@1064, high reflectivity mirror at $1064\ \text{nm}$; BS, beam splitter; HWP, half-waveplate; L, lens; M, mirror; DM, dichroic mirror; BSP, beam sampler; PD, photodiode; PA, preamplifier; FTIR, Fourier-transform infrared; HgCdTe, mercury cadmium telluride detector.

The length, width and thickness of the fan-out PPLN crystal used in our experiment are 40 mm, 16 mm and 0.5 mm, respectively. The poling period of the crystal is able to change from 24 μm to 28 μm continuously by mechanical translation. In order to avoid the influence due to external temperature changes during the experiment, the temperature of the crystals was maintained at 40°C above room temperature. The dichroic mirrors DM1 and DM2 are designed to separate the pump and signal waves, respectively, from the idler wave transmitting the mirrors. DM1 has high reflectivity ($R > 99\%$) for the pump wave and 99% transmission for the signal wave. DM2 has high reflectivity ($R > 99\%$) for the signal wave and high reflectivity ($R > 95\%$) for the pump wave. Both dichroic mirrors have 85% transmission for the idler wave.

To achieve the robust and stable operation of cw OPO, we applied the modified PDH scheme for cavity stabilization [28]. We notice that cw OPO stabilized by the modified PDH technique shows very good performance for power and wavelength stability. We utilized the frequency modulation function of our pump laser, which contains a piezo-actuator (PZT) on the laser crystal. The frequency-modulated pump laser reflected from the cavity is detected with an InGaAs photodiode (PD) and converted to a low-noise voltage signal by a preamplifier (PA). After demodulation of the converted signal using a lock-in amplifier, the error signal for the PID controller is obtained. The output signal from the PID controller is amplified and fed back to the PZT attached on the backside of the mirror M2 to vary the cavity length of the OPO. After the robust cw operation is achieved, the idler wavelength is monitored by using a FTIR spectrometer and the idler output power is measured by using a HgCdTe detector whose responsivity is calibrated. The sampling light for the FTIR was guided by InF₃ optical fiber. In order to block the residual signal and pump waves, an additional long-pass filter was used in front of the idler measurement devices.

III. EXPERIMENTAL RESULTS

Figure 2 shows (a) the wavelength tuning curve calculated using the temperature-dependent Sellmeier equation for a MgO:PPLN crystal, and (b) the wavelength-tunable idler spectra measured by using the FTIR spectrometer, combined in steps of 100 nm [29]. From Fig. 2(a), the wavelength of the idler is expected to be tunable from 4500 nm to 5500 nm by varying the poling periods from 24.5 μm to 27.3 μm . As shown in Fig. 2(b), we experimentally confirmed the widely tunable idler spectra by changing the fan-out designed period of the PPLN crystal from 24 μm to 28 μm . The spectral resolution of the FTIR spectrometer used in this measurement was 0.25 cm^{-1} . The spectra in Fig. 2(b) are normalized for better comparison at different set wavelengths. We note that the noise floor of the idler spectrum gradually increases as it approaches the limit of the operation range of the spectrometer used. The measured idler spectra in Fig. 2(b) show that our cw OPO is working well in the single longitudinal mode and successfully tuned up to a wavelength of 5.3 μm . Since the OPO cavity stabilization is performed using the PDH method, the stable idler spectra above 5.0 μm can be measured for a few minutes. In addition, in order to avoid perturbations from air convection and external vibration, the experimental setup was isolated from the surrounding environment by wrapping the optical table. Therefore, without external perturbation, our cw OPO is expected to have long-term stability over tens of minutes.

Figure 3 shows the measured output power characteristics at the idler wavelength of (a) 4.9 μm and (b) 5.2 μm as a function of the incident pump power. Each data point was averaged 10 times with a calibrated HgCdTe detector. The symbols represent the experimental data measured at the pump power set in the increasing (square) and decreasing (circle) order. The solid and dashed lines show the theoretical prediction based on the best fit of the conversion efficiency formula for a doubly resonant OPO

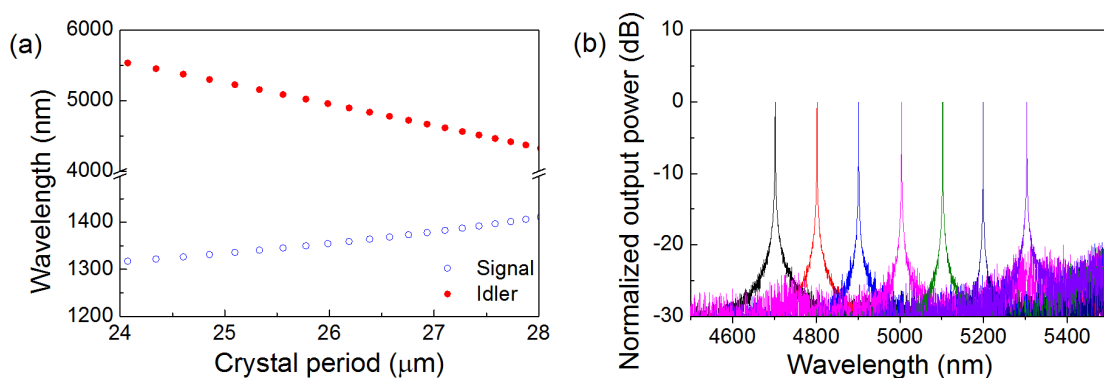


FIG. 2. (a) The calculated wavelength tuning curve with temperature dependent Sellmeier equation corresponding to the dispersion relations for a 5 mol% MgO-doped congruent PPLN crystal. (b) The wavelength-tunable idler spectra measured by FTIR spectrometer in steps of 100 nm. These spectra were obtained by changing the poling period of the fan-out grating MgO:PPLN crystal from 24 μm to 28 μm .

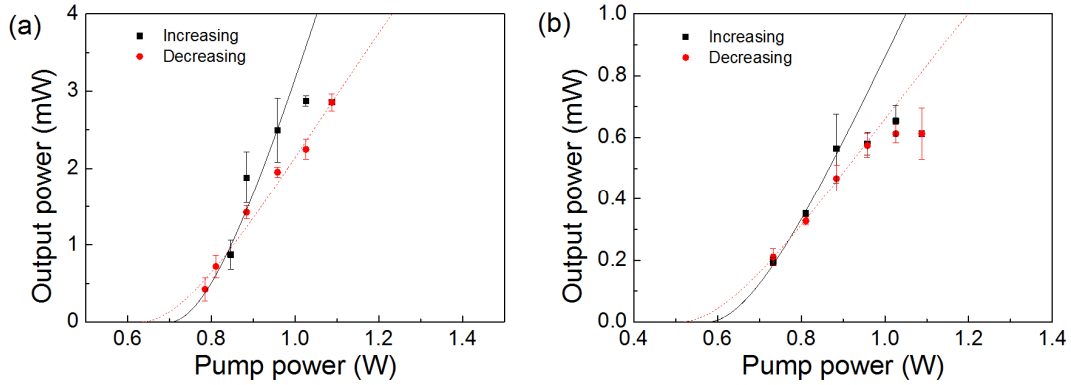


FIG. 3. Output power characteristics of the cw OPO at idler wavelength of (a) 4.9 μm and (b) 5.2 μm as a function of the pump power. The symbols corresponding to squares and circles indicate the measured results with increasing and decreasing pump power, respectively. Theoretical fittings resulted from the conversion efficiency formula using a Gaussian field were performed to the experimental data for the case of increasing (solid line) and decreasing (dashed line) pump power.

(DRO) with Gaussian field [3]

$$\eta = \frac{4}{N_{DRO}} (\sqrt{N_{DRO}} - \ln \sqrt{N_{DRO}} - 1), \quad (1)$$

where N_{DRO} is defined as the ratio P_{pump}/P_{th} of the incident pump power P_{pump} and the threshold pump power P_{th} . As a result of the fit, we obtain the threshold pump powers separately for pumping in the increasing and decreasing order. We confirm that the output power shows the bistability, which is observable in the cw OPOs with strong thermal lensing effect [14, 30, 31]. Thermal lensing effect is caused by the absorption of pump, signal and idler that occur inside the nonlinear crystal. In our case, it is assumed that the pump and signal waves are strongly absorbed inside the crystal because the pump-enhanced cavity is configured in the OPO setup. In addition, due to the high absorption of idler wave inside the crystal in the wavelength range above 4 μm , we expect that the absorption of the idler also contributed to the thermal lensing effect.

Figure 4 shows the threshold pump power of the OPO as a function of the idler wavelength in a range from 4.7 μm to 5.3 μm . The black filled square and circle symbols correspond to the experimentally determined values for pumping in the increasing and decreasing order, respectively, as representatively shown in Fig. 3. We notice that the threshold pump power for pumping in the increasing order is generally higher than that for pumping in the decreasing order. This result also seems to be caused by the thermal lensing effect has been observed in other papers [30]. To compare the experimentally determined results with the theoretical expectation, we calculated the threshold pump power based on two data sets of the OPO cavity mirrors: the first set was the spectral transmission data provided by the manufacturer (hollowed squares in Fig. 4), and the second set was the fixed transmission of 85% assumed to be spectrally independent (hollowed circles in Fig. 4). The theoretical calculation was based on the equation for a

triply resonant OPO [32]:

$$P_{th} = \frac{|\ln[(1-T_{p1})(1-T_{p2})(1-\alpha_p)^2]|}{2T_{p1}} \epsilon_0 V \times \left(\frac{n_s n_i n_p}{d_{eff}} \right)^2 \frac{\kappa_s \kappa_i \kappa_p}{\omega_s \omega_i}. \quad (2)$$

Here, α_p is the passive loss per half-roundtrip for pump wave, ϵ_0 is the permittivity, V is the mode volume of the cavity, and d_{eff} is the effective nonlinear coefficient. The n , κ , and ω denote the temperature-dependent refractive index of the crystal, the cavity loss parameter, and the angular frequency of the wave, respectively. The subscripts s, i, and p indicate the signal, idler, and pump waves, respectively. T_{p1} and T_{p2} are the transmittance of the input and output mirrors for the pump wave.

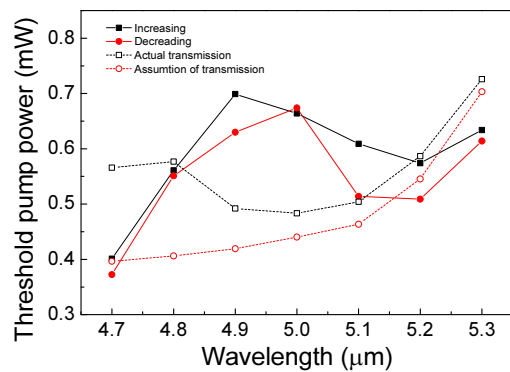


FIG. 4. The threshold pump power of cw OPOs as a function of idler wavelength. The symbols corresponding to filled squares and circles mean the estimated threshold values from the fitted experimental data according to increasing and decreasing pump power, respectively. The hollowed squares represent the calculated threshold values P_{th} on actual transmission data of the mirrors for idler wave, and the hollowed circles indicate P_{th} on the assumption that the transmission of the idler wave was constant at 85% on average.

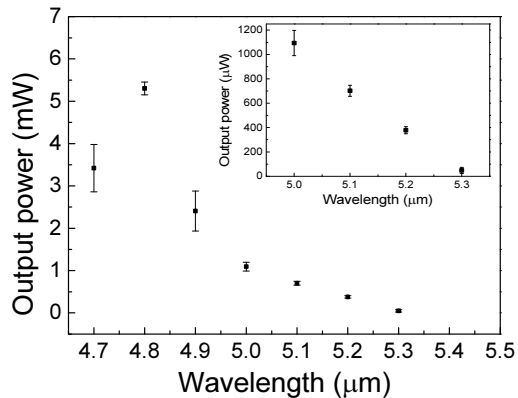


FIG. 5. The measured output power of the cw OPO as a function of idler wavelength. The inset in Fig. 5 denotes the detailed results of measured output power at idler wavelength above 5.0 μm . The maximum output power was 5.3 mW at idler wavelength of 4.8 μm , and the idler output power at 5.3 μm was measured to be approximately 50 μW .

The two results of the calculation plotted in Fig. 4 as the hollowed squares and circles show a difference at wavelengths near 4.8 μm , but the same tendency of a rapid increase at wavelengths above 5.0 μm . Considering the inaccuracy of the parameters used for the calculation, the overall agreement between the experimentally determined and the calculated results of the threshold pump power in Fig. 4 is satisfactory. This indicates that our cw OPO is close to the optimal realization of the theoretical prediction.

Figure 5 shows the idler output power as a function of wavelength measured in a step of 100 nm at a fixed pump power of 1.1 W. At a wavelength of 4.8 μm , the maximum output power is measured to be 5.3 mW. At the wavelengths longer than 4.8 μm , the output power rapidly decreases, which confirms the increasing absorptive property of the PPLN crystal in the long wavelength range [17]. The inset in Fig. 5 shows the measured output power above 5.0 μm in a magnified scale. In order to measure the radiant power smaller than 1 mW at wavelengths longer than 5.0 μm , we calibrated the responsivity of the HgCdTe detector by comparison with a pyroelectric radiometer at a wavelength of 4.8 μm where the OPO power is at its maximum. The linearity of the HgCdTe detector from the mW-range down to the μW -range as well as the spectrally independent responsivity in a wavelength range from 4.5 μm to 5.5 μm are assumed from the specifications of the manufacturer. As a result, the output power at a wavelength of 5.3 μm is measured to be approximately 50 μW . As shown in Fig. 2(b), we confirmed that this value at 5.3 μm was enough strong to observe the spectral characteristics of the idler output by using a conventional FTIR spectrometer.

IV. CONCLUSION

In conclusion, we presented a cw OPO based on a MgO:PPLN crystal, which can be stably operated at a wavelength as long as 5.3 μm . By using a fan-out grating design, the idler wavelength of the OPO pumped at 1064 nm could be continuously tuned from 4.7 μm to 5.3 μm . The output powers with increasing and decreasing pump power were measured as a function of idler wavelength. In the measurement of output power characteristics, we observed the bistability of the output power characteristics according to the pump power that is mainly caused by the thermal effects. The threshold pump power varied from 0.4 W to 0.7 W depending on wavelength, which was comparable with the theoretical calculations. When the PPLN crystal was pumped with a power of 1.1 W, we observed that the output powers of the cw OPO at longer wavelength than 4.8 μm were sharply reduced due to the strong absorption in the crystal. The maximum output power was measured to be 5.3 mW at a wavelength of 4.8 μm . The calibrated HgCdTe was used to measure the output power of 50 μW at a wavelength of 5.3 μm , which was sufficient to measure a single mode spectrum with a conventional FTIR spectrometer. Therefore, our results suggest the development of a continuous tunable, narrow linewidth mid-infrared cw OPO at wavelengths longer than 5.0 μm , which is useful for a variety of applications such as performance evaluation of mid-infrared spectrometer and mid-infrared spectroscopy.

ACKNOWLEDGMENT

This work was supported by the National Research Foundation of Korea (NRF) grant funded by the Korea government (MSIT) (2015M1A3A3A03027287, Development of performance evaluation technologies for gamma-ray, neutron and mid-IR spectrometer) and in part by the Korea Research Institute of Standards and Science project ‘Establishment of National Physical Measurement Standards and Improvements of Calibration/Measurement Capability’, grants 19011041.

REFERENCES

1. J. A. Giordmaine and R. C. Miller, “Tunable coherent parametric oscillation in LiNbO_3 at optical frequencies,” *Phys. Rev. Lett.* **14**, 973-976 (1965).
2. K. Devi, S. C. Kumar, and M. Ebrahim-Zadeh, “Tunable, continuous-wave, ultraviolet source based on intracavity sum-frequency-generation in an optical parametric oscillator using BiB_3O_6 ,” *Opt. Express* **21**, 24829-24836 (2013).
3. R. L. Sutherland, *Handbook of Nonlinear Optics*, 2nd ed. (Marcel Dekker, New York, 2003), Chapter 3.
4. L. E. Myers, R. C. Eckardt, M. M. Fejer, R. L. Byer, W. R. Bosenberg, and J. W. Pierce, “Quasi-phase-matched optical parametric oscillators in bulk periodically poled LiNbO_3 ,”

- J. Opt. Soc. Am. B **12**, 2102-2116 (1995).
5. I. Shoji, T. Kondo, A. Kitamoto, M. Shirane, and R. Ito, "Absolute scale of second-order nonlinear-optical coefficients," J. Opt. Soc. Am. B **14**, 2268-2294 (1997).
 6. L. E. Myers, G. D. Miller, R. C. Eckardt, M. M. Fejer, R. L. Byer, and W. R. Bosenberg, "Quasi-phase-matched 1.064- μm -pumped optical parametric oscillator in bulk periodically poled LiNbO₃," Opt. Lett. **20**, 52-54 (1995).
 7. T. J. Kulp, S. E. Bison, R. P. Bambha, T. A. Reichardt, U.-B. Goers, K. W. Aniolek, D. A. V. Kliner, B. A. Richman, K. M. Armstrong, R. Sommers, R. Schmitt, P. E. Powers, O. Levi, T. Pinguet, M. Fejer, J. P. Koplow, L. Goldberg, and T. G. McRae, "The application of quasi-phase-matched parametric light sources to practical infrared chemical sensing systems," Appl. Phys. B **75**, 317-327 (2002).
 8. A. K. Y. Ngai, S. T. Persijn, G. V. Basum, and F. J. M. Harren, "Automatically tunable continuous-wave optical parametric oscillator for high-resolution spectroscopy and sensitive trace-gas detection," Appl. Phys. B **85**, 173-180 (2006).
 9. S. Zaske, D.-H. Lee, and C. Becher, "Green-pumped cw singly resonant optical parametric oscillator based on MgO:PPLN with frequency stabilization to an atomic resonance," Appl. Phys. B **98**, 729-735 (2010).
 10. W. R. Bosenberg, A. Drobshoff, J. I. Alexander, L. E. Myers, and R. L. Byer, "Continuous-wave singly resonant optical parametric oscillator based on periodically poled LiNbO₃," Opt. Lett. **21**, 713-715 (1996).
 11. P. E. Powers, T. J. Kulp, and S. E. Bisson, "Continuous tuning of a continuous-wave periodically poled lithium niobate optical parametric oscillator by use of a fan-out grating design," Opt. Lett. **23**, 159-161 (1998).
 12. F. K. Tittel, D. Richter, and A. Fried, "Mid-infrared laser applications in spectroscopy," in *Solid-State Mid-Infrared Laser Sources*, Irina T. Sorokina Konstantin, L. Vodopyanov, ed. (Springer, Berlin, Heidelberg, 2003), pp. 458-529.
 13. B. M. Walsh, H. R. Lee, and N. P. Barnes, "Mid infrared lasers for remote sensing applications," J. Lumin. **169**, 400-405 (2016).
 14. A. Kosterev, G. Wysocki, Y. Bakhrkin, S. So, R. Lewicki, M. Fraser, F. Tittel, and R. F. Curl, "Application of quantum cascade lasers to trace gas analysis," Appl. Phys. B **90**, 165-176 (2008).
 15. M. W. Sigrist, "Mid-infrared laser-spectroscopic sensing of chemical species," J. Adv. Res. **6**, 529-533 (2015).
 16. K. K. Choi, J. N. Mait, J. M. Pellegrino, and G. L. Wood, "Optics research at the U.S. Army Research Laboratory," Appl. Opt. **56**, B103-B115 (2017).
 17. M. M. J. W. V. Herpen, S. E. Bisson, and F. J. M. Harren, "Continuous-wave operation of a single-frequency optical parametric oscillator at 4-5 μm based on periodically poled LiNbO₃," Opt. Lett. **28**, 2497-2499 (2003).
 18. M. Vainio, J. Peltola, S. Persijn, F. J. M. Harren, and L. Halonen, "Thermal effects in singly resonant continuous-wave optical parametric oscillators," Appl. Phys. B **94**, 411-427 (2009).
 19. J. Kiessling, R. Sowade, I. Breunig, K. Buse, and V. Dierolf, "Cascaded optical parametric oscillations generating tunable terahertz waves in periodically poled lithium niobate crystals," Opt. Express **17**, 87-91 (2009).
 20. J. Krieg, A. Klemann, I. Gottbehüt, S. Thorwirth, T. F. Giesen, and S. Schlemmer, "A continuous-wave optical parametric oscillator around 5- μm wavelength for high-resolution spectroscopy," Rev. Sci. Instruments **82**, 063105 (2011).
 21. D. J. M. Stothard, I. D. Lindsay, and M. H. Dunn, "Continuous-wave pump-enhanced optical parametric oscillator with ring resonator for wide and continuous tuning of single-frequency radiation," Opt. Express **12**, 502-511 (2004).
 22. G. A. Turnbull, D. McGloin, I. D. Lindsay, M. Ebrahimzadeh, and M. H. Dunn, "Extended mode-hop-free tuning by use of a dual-cavity, pump-enhanced optical parametric oscillator," Opt. Lett. **25**, 341-343 (2000).
 23. M. A. Watson, M. V. O'Connor, P. S. Lloyd, D. P. Shepherd, D. C. Hanna, C. B. E. Gawith, L. Ming, P. G. R. Smith, and O. Balachninaite, "Extended operation of synchronously pumped optical parametric oscillators to longer idler wavelengths," Opt. Lett. **23**, 2106-2108 (2002).
 24. G. Robertson, M. J. Padgett, and M. H. Dunn, "Continuous wave singly resonant pump-enhanced type II LiB₃O₅ optical parametric oscillator," Opt. Lett. **19**, 1735-1737 (1994).
 25. S. Schiller, K. Schneider, and J. Mlynek, "Theory of an optical parametric oscillator with resonant pump and signal," J. Opt. Soc. Am. B **16**, 1512-1524 (1999).
 26. A. Carleton, D. J. M. Stothard, I. D. Lindsay, M. Ebrahimzadeh, and M. H. Dunn, "Compact, continuous-wave, singly resonant optical parametric oscillator based on periodically poled RbTiOAsO₄ in a Nd:YVO₄ laser," Opt. Lett. **28**, 555-557 (2003).
 27. I. D. Lindsay, D. J. M. Stothard, C. F. Rae, and M. H. Dunn, "Continuous-wave, pump-enhanced optical parametric oscillator based on periodically poled RbTiOAsO₄," Opt. Express **11**, 134-140 (2003).
 28. K. Schneider, P. Kramper, S. Schiller, and J. Mlynek, "Toward an optical synthesizer: a single-frequency parametric oscillator using periodically poled LiNbO₃," Opt. Lett. **22**, 1293-1295 (1997).
 29. O. Gayer, Z. Sacks, E. Galun, and A. Arie, "Temperature and wavelength dependent refractive index equations for MgO-doped congruent and stoichiometric LiNbO₃," Appl. Phys. B **91**, 343-348 (2008).
 30. S. T. Lin, Y. Y. Lin, Y. C. Huang, A. C. Chiang, and J. T. Shy, "Observation of thermal-induced optical guiding and bistability in a mid-IR continuous-wave, singly resonant optical parametric oscillator," Opt. Lett. **33**, 2338-2340 (2008).
 31. I.-H. Bae, H. S. Moon, S.-K. Kim, S. N. Park, and D.-H. Lee, "Self-guided operation of singly resonant continuous-wave optical parametric oscillator based on bulk MgO-doped PPLN," Appl. Phys. B **106**, 797-801 (2012).
 32. D.-H. Lee, M. E. Klein, and undefined K.-J. Boller, "Intensity noise of pump-enhanced continuous-wave optical parametric oscillators," Appl. Phys. B **66**, 747-753 (1998).